Supporting Information

An *in situ* derived MOF@In_2S_3 heterojunction stabilizes Co(II)-salicylaldimine for efficient photocatalytic formic acid dehydrogenation

Meijin Zhang [a], Wenting Lin [a], Liang Ma [a], and Yunhong Pi [a], Tiejun Wang [a]**

[a] School of Chemical Engineering and Light Industry, and Guangzhou Key Laboratory of Clean Transportation Energy and Chemistry, Guangdong University of Technology, Guangzhou 510006, P. R. China.

*Corresponding author. E-mail: piyunhong@gdut.edu.cn; tjwang@gdut.edu.cn

Table of contents

1. Experimental Section

1.1. Chemicals and Reagents.

Indium nitrate hydrate ($In(NO_3)_3 \cdot xH_2O$, 99.9%), 2-Aminoterephthalic Acid ($H_2BDC\text{-}NH_2$, 98%), N,N-dimethylformamide (DMF, 99.5%), Salicylaldehyde ($C_7H_6O_2$, 99%), Cobalt(II) perchlorate hexahydrate ($Co(ClO_4)_2 \cdot 6H_2O$, 98%), Iron(II) tetrafluoroborate hexahydrate ($Fe(BF_4)_2 \cdot 6H_2O$, 97%), ethanol (EtOH, 95%), Deuterium oxide (D_2O, 99.9%) were purchased from Aladdin Chemistry Co., Ltd. Thiourea (CH_4N_2S, 99.0%) was obtained from Damao Chemical Reagent Factory. N-N-Dimethylacetamide (DMA, 99.8%), Tetrahydrofuran (THF, 99.9%), Copper (II) chloride ($CuCl_2$, 99.8%), Nickel(II) chloride hexahydrate ($NiCl_2 \cdot 6H_2O$, 99.8%) were supplied from Shanghai Macklin Biochemical Co., Ltd. Methanol (MeOH) were purchased from Guanghua Chemicals. All the chemicals were used without further purification.

1.2. Solvothermal Synthesis of NH_2-MIL-68.

NH_2-MIL-68(In) was synthesized by a solvothermal process. Typically, $H_2BDC\text{-}NH_2$ (0.234 g) and $In(NO_3)_3 \cdot xH_2O$ (1.156 g) were dissolved in 12.4 ml of DMF and stirred for 10 min. The resulting clear solution was subsequently transferred into a 35 ml Pyrex glassware and retained at 125 °C for 5 h, yielding a faint yellow precipitate by centrifugation and washed thoroughly with DMF after cooling down temperature. Then the obtained product was immersed in anhydrous methanol for purification at 60 °C for 48 h to remove the guest molecules present in the pores, and finally centrifuged and dried overnight under vacuum at room temperature.

1.3. Post-Solvothermal Treatment for NH_2-MIL-68@In_2S_3.

The in-situ derived NH_2-MIL-68@In_2S_3 heterostructure was prepared with NH_2-MIL-68(In) obtained in previous step as precursor. Briefly, NH_2-MIL-68 (100 mg) was suspended in 15 ml ethanol in a 50 ml beaker followed by dropwise addition of a thiourea /ethanol solution (200 mg thiourea in 15 ml ethanol). The resulting mixture was stirred for 30 min and then transferred to a Teflon-lined autoclave, maintaining at 180 °C for 2 h. The solution was then cooled to room temperature, followed by filtration and washing with ethanol. Subsequently, the resulting product was purified in anhydrous ethanol at 60 °C for 48 h, and then collected before being dried overnight under vacuum at room temperature to afford NH_2-MIL-68@In_2S_3 as a dark yellow solid. Through the identical sulfidation process with extended reaction time (12 h), pure In_2S_3 with rod-like structure as NH_2-MIL-68 was also synthesized as comparison.[1]

1.4. Synthesis of Co-sal-NH_2-MIL-68@In_2S_3.

Co-sal-NH_2-MIL-68@In_2S_3 was constructed via a two-step post-synthetic process with formation of salicylaldimine moiety (sal-MOF) by salicylaldehyde modification and following metalation with cobalt salts to provide robust and highly active single-site solid catalytic centers. Firstly, 30 mg of as-obtained NH_2-MIL-68@In_2S_3 was dispersed into 40 ml of methanol in a flask under ultrasound, and 12 μl of salicylaldehyde was then added into the mixture, followed by reflux at 100 °C for 24 h. Afterwards, the precipitate was washed with abundant ethanol three times and dried under vacuum at room temperature overnight to give a light orange solid as sal-NH_2-MIL-68@In_2S_3. Subsequently, the obtained sal-NH_2-MIL-68@In_2S_3 (10.0 mg) was suspended in 2 ml THF in a vial, following with the addition of $Co(ClO_4)_2 \cdot 6H_2O$/THF

solution (2.73 μmol $Co(ClO_4)_2 \cdot 6H_2O$ in 2.0 ml THF). The mixture was stirred slowly overnight for 24 h and the resulting deep orange solid was centrifuged out of suspension and washed with THF 4-5 times to afford the final powdery Co-sal-NH_2-MIL-68@In_2S_3. ICP-OES analysis of the digested Co-sal-NH_2-MIL-68@In_2S_3 revealed a Co-loading of 4.3×10^{-3} *wt*%.

For comparison, M-sal-NH_2-MIL-68@In_2S_3 (M = Fe, Cu, Ni) were synthesized similarly as Co-sal-NH_2-MIL-68@In_2S_3 with the exception that $Co(ClO_4)_2$ was replaced by $Fe(BF_4)_2$, $CuCl_2$, or $NiCl_2$, respectively.

1.5. Characterization.

Powder X-ray diffraction (PXRD) data was collected on a MiniFlex 600 diffractometer using monochromatized Cu Kα radiation (λ= 0.15418 nm) source with a step size of 0.02° at 10° per minute. The Fourier-transform infrared (FTIR, Thermo-Filsher) spectroscopy measurements were conducted with Nicolet 6700 FTIR Spectrometric Analyzer using KBr pellets. The morphological study of the as-synthesized hybrid nanostructures was obtained through Scanning electron microscope (SEM, Hitach */SU8220), transmission electron microscopy (TEM, FEI, Thermo */Talos F200S). The interaction and chemical compositions of the composites were analyzed by X-ray photoelectron spectroscopy (XPS, ESCALAB 250Xi). UV–Vis diffused reflectance spectra (DRS) were carried out on a UV-Vis spectrophotometer (UV-2600i, Shimadzu, Japan), with $BaSO_4$ as a reflectance standard. An ASAP 2460 V2.01 apparatus (Micromeritics Instrument Corp., USA)

was applied to record the Brunauer-Emmett-Teller (BET) surface area and porous structure, with nitrogen adsorption and desorption isotherms of samples measured at 77 K after being degassed under vacuum at 150 °C for 6 h. Inductively coupled plasma-mass spectrometry (ICP-OES) data was recorded with an Agilent 730 ICP-OES. The photoluminescence spectra (PL) were observed on a fluorescence spectrometer (FLS 980, Edinburgh, England) with an excitation wavelength of 450 nm. The Mott-Schottky curves, photocurrent response and Cyclic voltammetry were performed on an electrochemical workstation (CHI660D) with a three-electrode cell with graphite rod as a counter electrode, Ag/AgCl as a reference electrode, and an electrolyte (0.5 M Na_2SO_4 aqueous solution at pH=7). Electron spin-resonance (ESR) spectra were carried out with Bruker EMXnano at room temperature. Amounts of H_2 and CO etc. generated in the photocatalytic experiments were determined by gas chromatography (GC) using a GC9790PLUS with the Ar carrier gas and a TCD or FID detector.

1.6. Photocatalytic Hydrogen Evolution from Formic Acid.

The photocatalytic H_2 evolution from FA was carried out in an externally illuminated reaction vessel with a magnetic stirrer, with samples prepared in a 5.0 ml septum-sealed glass vial. In the standard reaction, each sample was made up to a volume of 2.00 ml, including 1.80 ml DMA, 10 μl FA, 0.20 ml H_2O, and 45 mg 1,3-dimethyl-2-phenyl-2,3-dihydro-1H-benzo[d]imidazole (BIH, 0.2 mmol) in addition to a certain amount of MOF catalyst. The sample vials were capped and sealed, and deoxygenated by bubbling nitrogen for 5 minutes to ensure complete removal of air. Keeping at room temperature, the solution was irradiated by a 300 W Xe lamp (PLS-

SXE300+＞420 nm) equipped with a cooling fan for 24 hours. After the hydrogen evolution reaction, the gas in the headspace of the vial is analyzed by GC to determine the amount of H_2 produced. TON of H_2 evolution reaction was calculated based on the amount of catalytic Co sites.

1.7. Recycle tests of Co-sal-NH_2-MIL-68@In_2S_3 catalyzed photocatalytic Hydrogen Evolution from Formic Acid.

Recycle tests on Co-sal-NH_2-MIL-68@In_2S_3 for photocatalytic hydrogen evolution from formic acid was carried out to demonstrate the stability and reusability of the present catalytic MOF system. Specifically, hydrogen evolution recycle reactions were conducted with Co-sal-NH_2-MIL-68@In_2S_3 catalyst (7.32 nmol Co site), and 45 mg BIH, in 10 μL FA + 1.8 mL DMA+0.2 mL H_2O, under ＞420 nm Xe lamp for 24 h. The solution was degassed with N_2 for 5 min before each run and 5 mg of BIH was added to the solution after each run.

1.8. Photoelectrochemical measurements.

The working photoelectrodes were prepared as follows: 4 mg of photocatalyst powders were dispersed in mixed solution containing 1 ml of THF and 40 μl of Nafion with ultrasound treatment for 30 min. Then the mixed solution was dropped and dried several times on Glassy carbon electrode (0.25×0.25 π cm^2). The photocurrent response curves, linear sweep voltammetry (LSV), Cyclic voltammograms (CV), electrochemical impedance spectroscopy (EIS) and Mott-Schottky plots were accomplished in an electrochemical workstation using three electrode system, in which a graphite rod, a saturated Ag/AgCl and the prepared photoelectrode were used as counter electrode, reference electrode and working

electrode, respectively. A 300 W Xe lamp was used as light sources and Na_2SO_4 aqueous solution (0.5 M) was chose as electrolyte (CV features was conducted in 10 ml 0.1 M TBAH (Tetrabutyl-ammonium hexafluorophosphate) /DMA solution with 1 ml H_2O with a scan rate of 50 mV/s.). The Mott-Schottky measurement was conducted in the potential range from -1.2 to 0 V with the frequency of 0.5 and 1.0 kHz, respectively.

1.9. Calculation of turnover number (TON).

The calculation of turnover number (TON) over Co-sal-NH_2-MIL-68@In_2S_3 was using the following equation:

$$\text{TON} = \frac{\text{moles of evolved products gas}}{\text{moles of active sites on photocatalysts}}$$

1.10. Calculation of apparent quantum efficiency (AQE).

The apparent quantum efficiency (AQE) for H_2 evolution was evaluated by a 300 W Xe lamp (PLS-SXE300+). The monochromatic wavelength of light (λ) was set at 420 nm. The amount of generated H_2 was analyzed by GC after 24 hours of light irradiation. AQE under the different wavelengths were calculated by the following equation:

$$AQE(\%) = \frac{Ne}{Np} = \frac{(2 \times number\ of\ evolved\ H_2\ molecules)}{(number\ of\ incident\ photons)}$$

2. Supplementary Figures of Material Characterizations

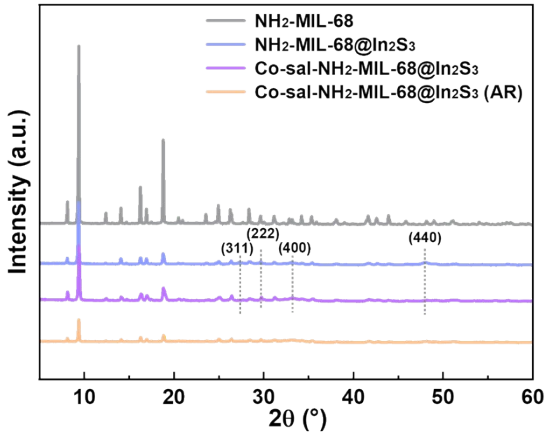

Figure S1. PXRD patterns of NH_2-MIL-68, NH_2-MIL-68@In_2S_3 and Co-sal-NH_2-MIL-68@In_2S_3 before and after photocatalytic H_2 evolution from FA reaction.

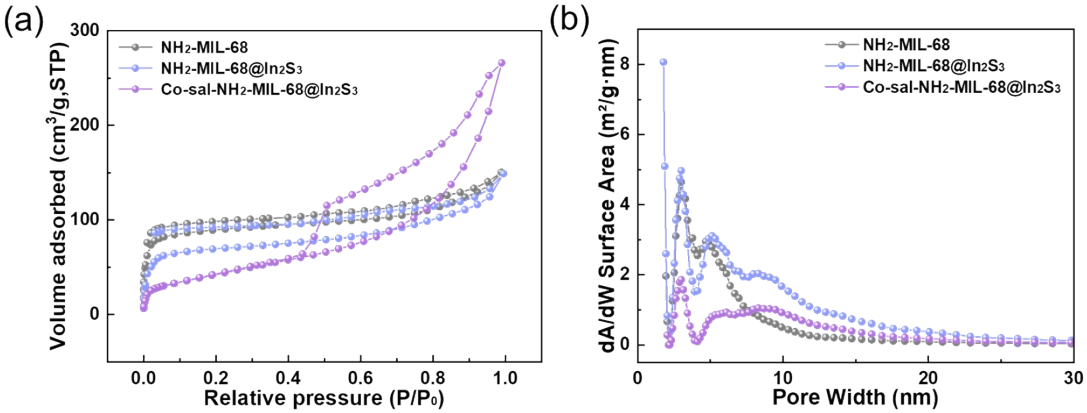

Figure S2. a) N_2 adsorption isotherms and b) pore size distribution of NH_2-MIL-68, NH_2-MIL-68@In_2S_3 and Co-sal-NH_2-MIL-68@In_2S_3.

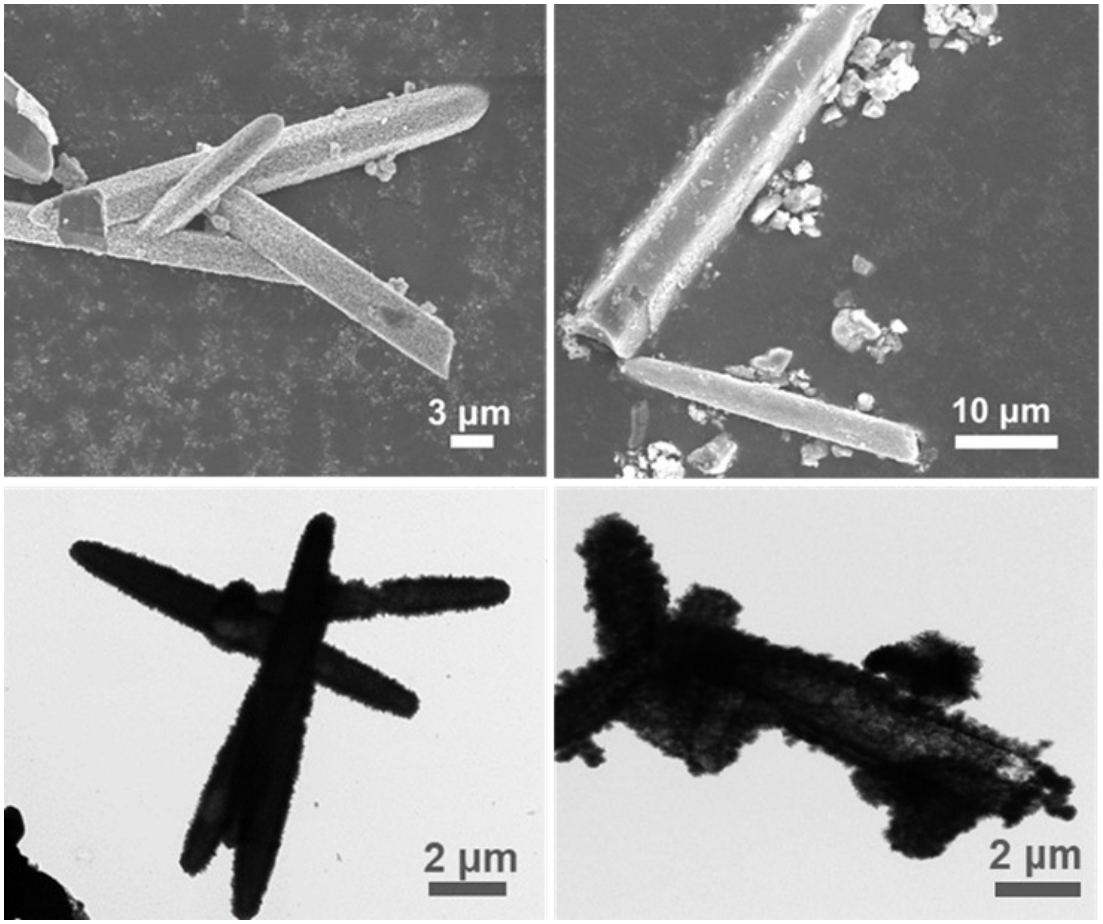

Figure S3. SEM and TEM images of Co-sal-NH_2-MIL-68@In_2S_3 after photocatalytic H_2 evolution from FA reaction.

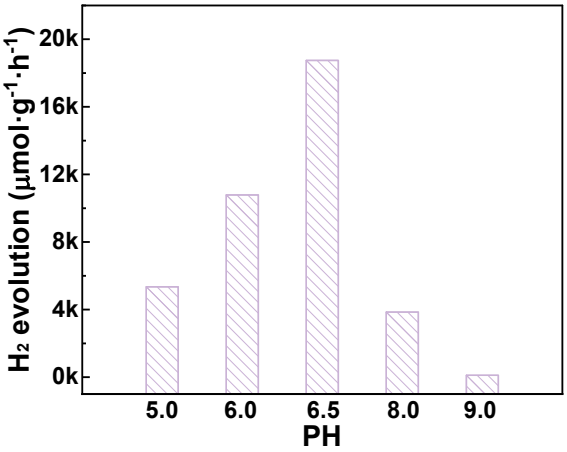

Figure S4. Photocatalytic H_2 generation with various pH values.

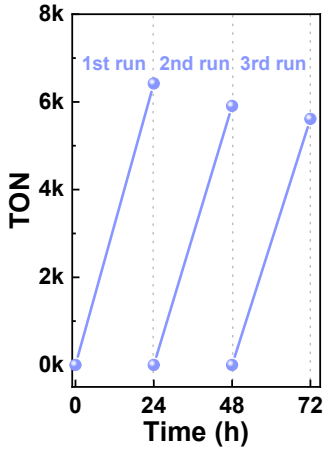

Figure S5. Recycle Test of Co-sal-NH_2-MIL-68@In_2S_3 catalyzed photocatalytic H_2 evolution in three consecutive runs.

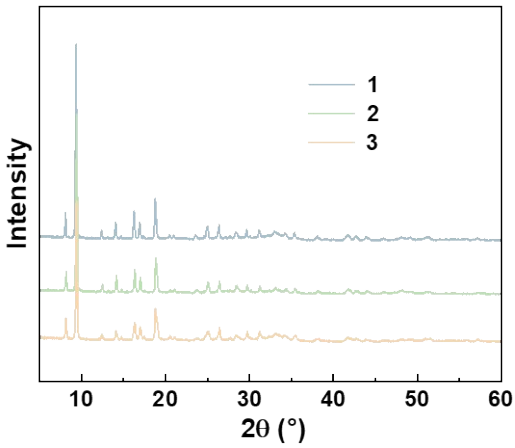

Figure S6. XRD of Co-sal-NH_2-MIL-68@In_2S_3 synthesized from three parallel experiments.

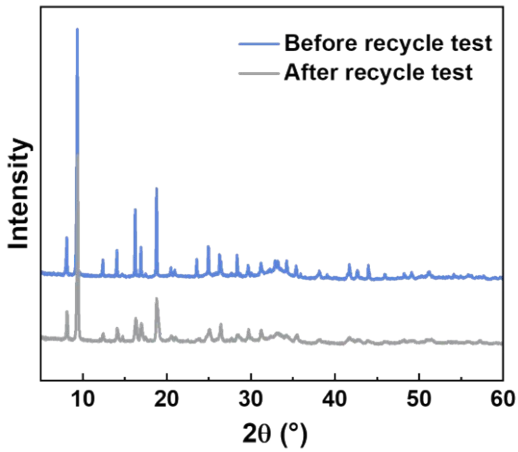

Figure S7. XRD patterns before and after the recycle test of Co-sal-NH_2-MIL-68@In_2S_3 catalyzed photocatalytic H_2 evolution.

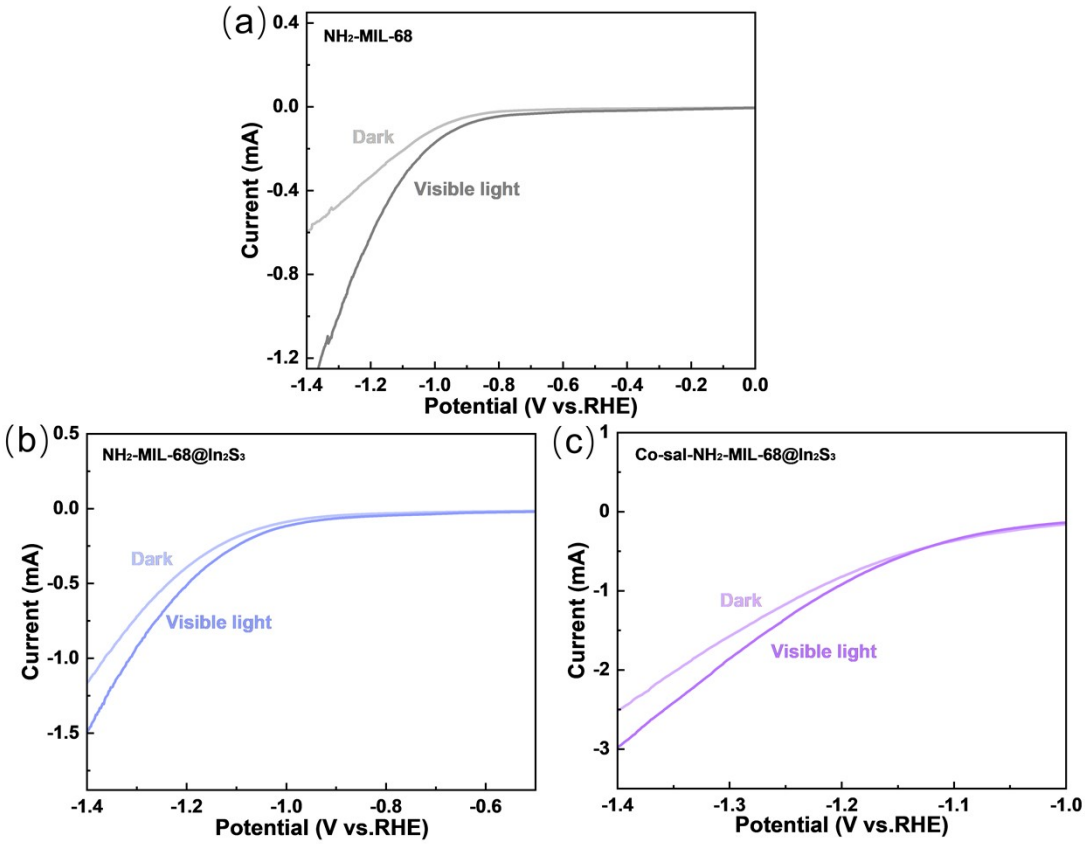

Figure S8. Current–voltage curve of NH_2-MIL-68 (a), NH_2-MIL-68@In_2S_3 (b) and Co-sal-NH_2-MIL-68@In_2S_3 (c) in a three-compartment cell under visible-light illumination ($\lambda > 420$ nm).

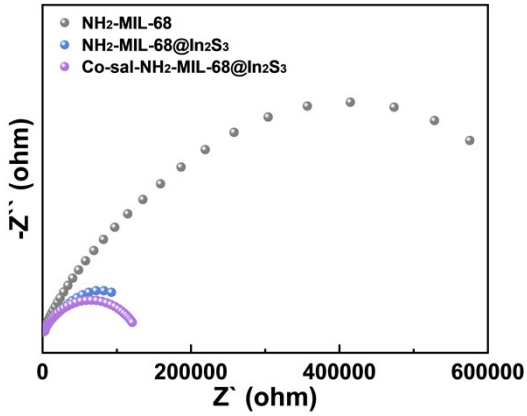

Figure S9. EIS Nyquist plots of the as-prepared NH_2-MIL-68, NH_2-MIL-68@In_2S_3 and Co-sal-NH_2-MIL-68@In_2S_3.

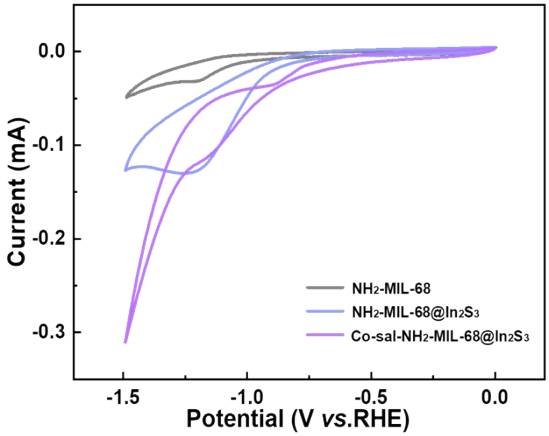

Figure S10. CV scans of the as-prepared NH_2-MIL-68, NH_2-MIL-68@In_2S_3 and Co-sal-NH_2-MIL-68@In_2S_3.

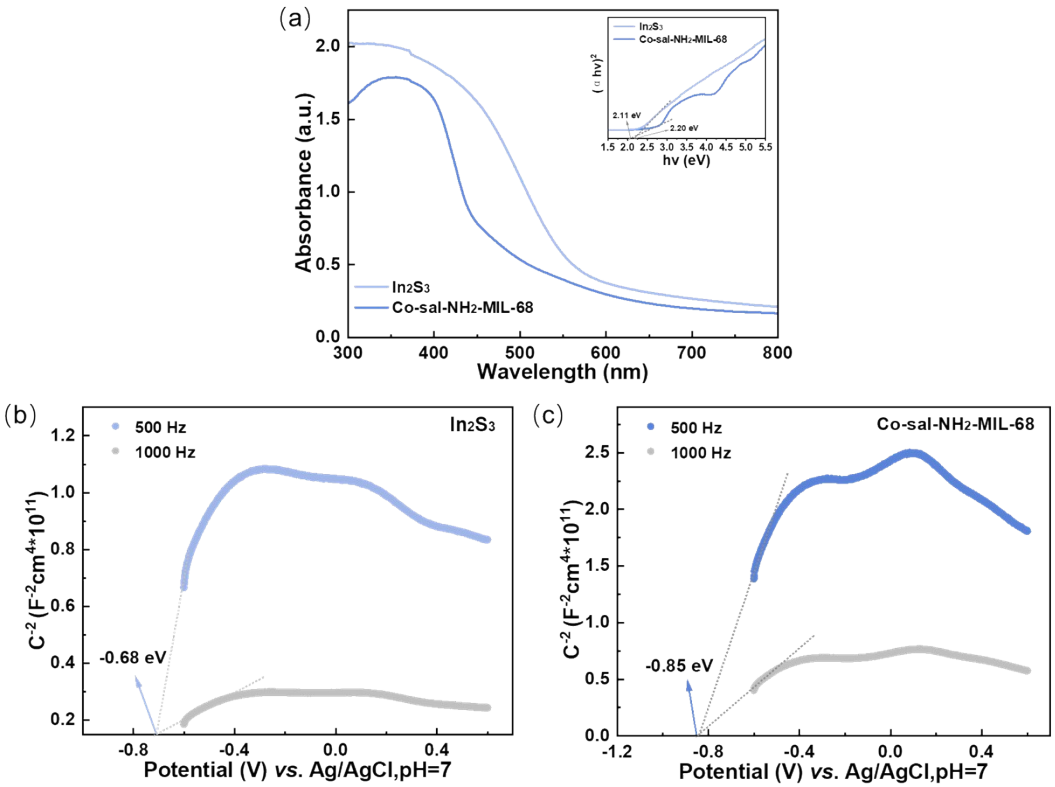

Figure S11. a) UV-vis DRS spectra and plots of (αhv) 1/2 *vs*. photon energy of MOF-derived In_2S_3, and Co-sal-NH_2-MIL-68; b-c) Mott−Schottky plots of MOF-derived In_2S_3 and Co-sal-NH_2-MIL-68.

3. Supplementary Tables

Table S1. BET surface area, pore volume and pore diameter of NH_2-MIL-68, NH_2-MIL-68@In_2S_3 and Co-sal-NH_2-MIL-68@In_2S_3

Sample	BET ($m^2 \cdot g^{-1}$)	BJH pore volume ($cm^3 \cdot g^{-1}$)	BJH Desorption average pore diameter (nm)
NH_2-MIL-68	368	0.08	6.89
NH_2-MIL-68@In_2S_3	274	0.18	10.47
Co-sal-NH_2-MIL-68@In_2S_3	133	0.09	12.02

Table S2. Condition screening of solvent amounts of photocatalytic H_2 evolution catalyzed by Co-sal-NH_2-MIL-68@In_2S_3.[a]

Entry	Sacrificial Agent	DMA / ml	H_2O / ml	FA / μl	Efficiency / $\mu mol g^{-1} h^{-1}$
1	BIH	2.0	-	-	0
2	BIH	2.0	-	10	1029
3	BIH	1.95	0.05	10	2900
4	BIH	1.90	0.10	10	15087
5	BIH	1.75	0.25	10	18370
6	**BIH**	**1.80**	**0.20**	**10**	**18746**
7	BIH	1.80	0.20	-	3
8	BIH	1.80	0.20	20	1684
9	BIH	1.80	0.20	30	371
10	BIH	1.80	0.20	50	143
11[b]	BIH	1.80	0.20	10	0
12[c]	BIH	1.80	0.20	10	11176
13[d]	BIH	1.80	0.20	10	1309
14[e]	BIH	1.80	0.20	10	1159
15[f]	BIH	1.80	0.20	10	607

[a] Unless noted, photocatalytic H_2 evolution from FA reactions were conducted with Co-sal-NH_2-MIL-68@In_2S_3 catalyst (7.32 nmol Co site), and 45 mg BIH under visible-light illumination ($\lambda > 420$ nm) for 24 h. [b] Catalyst: Co-sal-NH_2-MIL-68@In_2S_3 (0 nmol Co site). [c] Catalyst: Co-sal-NH_2-MIL-68@In_2S_3 (3.66 nmol Co site). [d] Catalyst: Co-sal-NH_2-MIL-68@In_2S_3 (10.98 nmol Co site). [e] Catalyst: Co-sal-NH_2-MIL-68@In_2S_3 (14.64 nmol Co site). [f] Catalyst: Co-sal-NH_2-MIL-68@In_2S_3 (21.96 nmol Co site).

Table S3. Control experiments of photocatalytic H_2 evolution from FA. [a]

Entry	Catalyst	Efficiency ($\mu molg^{-1}h^{-1}$)	TON	H_2 Selectivity (%)
1	$Co(ClO_4)_2$ + sal-NH_2-MIL-68	437	143	97.8
2	$Co(ClO_4)_2$ + sal-NH_2-MIL-68@In_2S_3	10277	3369	99.9
3	Co-sal-NH_2-MIL-68+In_2S_3	1709	560	99.4
4	$Co(ClO_4)_2$+ NH_2-MIL-68@In_2S_3	5731	1879	99.8
5	$Co(ClO_4)_2$+ sal-NH_2-MIL-68+In_2S_3	1017	667	99.2
6	**Co-sal-NH_2-MIL-68@In_2S_3**	**18746**	**6146**	**99.9**

[a] Unless noted, photocatalytic H_2 evolution from FA reactions were conducted with MOF or control catalysts (containing 7.32 nmol Co site), and 45 mg BIH, in 10 μl FA + 1.80 ml DMA+0.2 mL H_2O, under visible-light illumination (λ > 420 nm) for 24 h.

Table S4. Parallel experiment of photocatalytic H_2 evolution from FA. [a]

Entry	Efficiency ($\mu molg^{-1}h^{-1}$)	TON	H_2 Selectivity (%)
1	18746	6146	99.9
2	18023	5908	99.9
3	18713	6134	99.9

[a] Unless noted, photocatalytic H_2 evolution from FA reactions were conducted with MOF or control catalysts (containing 7.32 nmol Co site), and 45 mg BIH, in 10 μl FA + 1.80 ml DMA+0.2 mL H_2O, under visible-light illumination (λ > 420 nm) for 24 h.

Table S5. Photocatalytic activities of salicylaldimine moiety stabilized Cu, Fe, Ni catalytic sites. [a]

Sample	TON	H_2 Selectivity (%)
Cu-sal-NH_2-MIL-68@In_2S_3	367	99.4
Fe-sal-NH_2-MIL-68@In_2S_3	1169	99.8
Ni-sal-NH_2-MIL-68@In_2S_3	5724	99.7

[a] Reactions were conducted with MOF catalysts (containing 8 nmol Cu/ Fe /Ni site), and 45 mg BIH, in 10 μl FA + 1.80 ml DMA + 0.2 ml H_2O, under visible-light illumination (λ > 420 nm) for 24 h.

Table S6. Comparison of activities over different systems for photocatalytic H_2 evolution from FA

System	Catalyst	Light source	Sacrificial Agent	Reaction Conditions	Efficiency ($\mu mol g^{-1} h^{-1}$)	TON	Year
Carbon material	PdAg@g-C_3N_4	Xe lamp > 400 nm	/	HCOOH (1 M)	552000	315	2018[2]
	Au_xPd_y/CNS	Xe lamp > 420 nm	/	1M HCOOH/HCOONa (4:1)	72000	170	2019[3]
	$Ag_{0.1}Pd_{0.9}$/2D CNNs	Xe lamp > 400 nm	/	HCOOH/HCOONa (3:1)	2316000	61	2020[4]
	AuPdNi/DCN-10-APTS	Xe lamp > 420 nm	EDTA-2Na	HCOOH/HCOONa (1:1)	1493000	5148	2021[5]
	PF-$Mo_{1.98}C_{1.02}$	Sunlight	/	HCOOH/HCOONa (1:3)	25800	-	2021[6]
Semiconductor	QD-MPA/$CoCl_2$	Xe lamp > 420 nm	/	HCOOH/HCOONa	120000	10223	2015[7]
	CdS/Fe-salen	Xe lamp > 420 nm	/	H_2O/CH_3CN (3:1) PH 3.5	150000	1125	2020[8]
	FeP@CdS	Xe lamp > 420 nm	/	HCOOH (4 M) PH 3.5	278000	311	2021[9]
	NiCoP@CdS	Xe lamp > 420 nm	/	HCOOH (4 M) PH 3.5	354000	1684	2021[10]
Oxide	Au@SiO_2-Pt	Xe lamp > 420 nm	/	HCOOH/H_2O (1:100)	50 $\mu mol g^{-1}$Pt	9	2021[11]
	BFO	250 nm < Xe lamp < 500 nm	/	HCOOH (0.1 M) PH 3	30	-	2018[12]
Polymer	PCN-520-F	LED lamp	/	5%HCOOH 0.5%Pt	1600	63	2020[13]
MOF	Au@Pd/UiO-66($Zr_{85}Ti_{15}$)	Xe lamp > 420 nm	/	H_2O/HCOOH (100:3)	357100	400	2016[14]
	CdS@ZIF-8	Xe lamp > 420 nm	/	HCOOH/HCOONa (3:1) H_2PtCl	900	-	2016[15]
	Co-sal-NH_2-MIL-68@In_2S_3	**Xe lamp > 420 nm**	**BIH**	**DMA/H_2O/FA (180:20:1)**	**18746**	**6146**	**This work**

References

1. Q. Hou, X. Li, et al, Construction of In_2S_3@NH_2-MIL-68(In)@In_2S_3 Sandwich Homologous Heterojunction for Efficient CO_2 Photoreduction. *Ind. Eng. Chem. Res.* **2020**, 59, 47, 20711.

2. X. Du, J. Sun, et al. Photocatalytic dehydrogenation of formic acid promoted by a superior PdAg@g-C_3N_4 Mott–Schottky heterojunction. *Nanoscale Adv.*, **2021**, 3, 4447.

3. D. Yu, L. Li, et al. Plasmonic AuPd-based Mott-Schottky photocatalyst for synergistically enhanced hydrogen evolution from formic acid and aldehyde. *Appl. Catal. Environ.* B, **2019**, 251, 66.

4. C. Wan, L. Zhou, et al. Boosting visible-light-driven hydrogen evolution from formic acid over AgPd/2Dg-C_3N_4 nanosheets Mott-Schottky photocatalyst. *Chem. Eng. J.*, **2020**, 396, 125229.

5. G. Huang, X. Gu, et al. Alkylamine-Grafted Organic Semiconductors with Plasma-Induced Defects as Electron Promoters of CO-Resistant Pd-Based Nanoparticles for Efficient Light-Driven On-Demand H_2 Generation. *ACS Appl. Energy Mater.*, **2021**, 4, 704.

6. C. Lv，P. Lou, et al. Efficient hydrogen production via sunlight-driven thermal formic acid decomposition over a porous film of molybdenum carbide. *J. Mater. Chem. A*, **2021**,9, 22481.

7. Kuehnel, M.F., Wakerley, D.W., et al. Photocatalytic Formic Acid Conversion on CdS Nanocrystals with Controllable Selectivity for H_2 or CO. *Angew. Chem. Int. Ed.*, **2015**, 54, 9627.

8. R. M. Irfan, T. Wang, et al. Homogeneous Molecular Iron Catalysts for Direct Photocatalytic Conversion of Formic Acid to Syngas (CO+H_2). *Angew. Chem. Int. Ed.*, **2020**, 59, 14818.

9. T. Wang, L. Yang, et al. CdS Nanorods Anchored with Crystalline FeP Nanoparticles for Efficient Photocatalytic Formic Acid Dehydrogenation. *ACS Appl. Mater. Interfaces*, **2021**, 13, 20, 23751.

10. H. Cao, T. Wang, et al. NiCoP nanoparticles anchored on CdS nanorods for enhanced hydrogen production by visible light-driven formic acid dehydrogenation. *Int. J. Hydrog. Energy*, **2021**, 46, 64, 32435.

11. X. Yuan, W. Zhen, et al. Plasmon Coupling Induced Hot Electrons for Photocatalytic Hydrogen Generation. *Chem. Asian J.* **2021**, 16, 3683.

12. W. Ramadan, R. Dillert, et al. Changes in the solid-state properties of bismuth iron oxide during the photocatalytic reformation of formic acid. *Catal. Today,* **2019**, 326, 22.

13. Y. Li, R. He, P. Han, et al. A new concept: Volume photocatalysis for efficient H_2 generation Using low polymeric carbon nitride as an example. *Appl. Catal. Environ. B,* **2020**, 279, 119379.

14. M. Wen, Kohsuke Mori, et al. Plasmonic Au@Pd Nanoparticles Supported on a Basic Metal−Organic Framework: Synergic Boosting of H_2 Production from Formic Acid. *ACS Energy Lett.*, **2017**, 2, 1, 1.

15. Zeng, M., Chai, Z., Deng, X. et al. Core–shell CdS@ZIF-8 structures for improved selectivity in photocatalytic H_2 generation from formic acid. *Nano Res.*, **2016**, 9, 2729.